Evidence for a Spatially-Modulated Superfluid Phase of ^{3}He under Confinement: Supplemental Material

Lev V. Levitin, Ben Yager, Laura Sumner, Brian Cowan, Andrew J. Casey, and John Saunders
Department of Physics, Royal Holloway University of London, Egham, Surrey, TW20 0EX, UK

Nikolay Zhelev, Robert G. Bennett, and Jeevak M. Parpia
Department of Physics, Cornell University, Ithaca, NY, 14853 USA
(Dated: 15 January 2019)

EXPERIMENTAL SETUP

The apparatus of this experiment is in most aspects identical to that used in Ref. [39] and described in its supplementary material. The main difference is the improved uniformity of the cavity, see Fig. S1, achieved through optimised nanofabrication, introduction of a partition wall and restricting the measurements to low pressure [41]. In addition the cell fill line was interrupted with a superfluid-leaktight cryogenic valve [41, 42] at 6 mK, to avoid gradual depletion of the ^{4}He film due to the fountain effect.

TEMPERATURE CORRECTION

The thermometry in our experimental setup is based on monitoring the temperature of the silver sinter heat exchanger with a ^{195}Pt NMR thermometer, calibrated against the ^{3}He melting curve. In recent work on a $D = 0.2\,\mu$m slab [43] the temperature gradient between silver sinter (at $T_{\rm Ag}$) and helium (at $T_{\rm He}$) in the heat exchanger was carefully determined for various surface ^{4}He coverages. With ^{4}He plating similar to the one used in this experiment, the correction was found to be

$$T_{\rm He}^{3.5} - T_{\rm Ag}^{3.5} = C, \tag{S1}$$

corresponding to thermal boundary resistance $R_{\rm K}(T) \propto 1/T^{2.5}$. The constant C in (S1), determined by heat leak

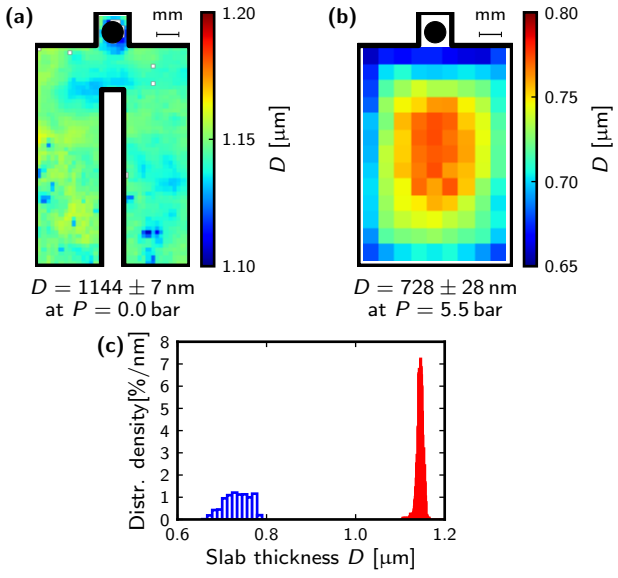

FIG. S1: Spectroscopic measurement of the thickness D of silicon-glass microfluidic cavities. The 1.1 μm cavity used in the experiment described here is compared to the 0.7 μm cavity from Refs. [32, 39], inflated under pressure necessary to stabilise the B phase. In the present work the slab uniformity is improved, one of the reasons being the partition wall in the middle of the cell [41].

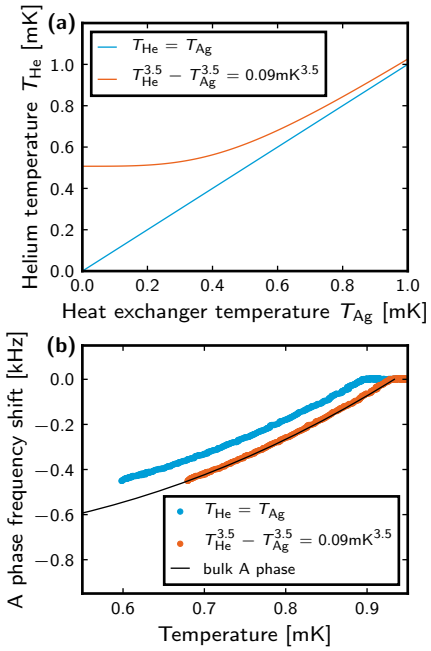

FIG. S2: Temperature correction. (a) Relationship between temperatures $T_{\rm He}$ and $T_{\rm Ag}$ of helium and silver sinter in the heat exchanger. (b) Frequency shift in the A phase is expected to have the bulk value, since the energy gap in the A phase is not suppressed in a slab with specular walls. This is found to be the case after the temperature correction. Here the bulk frequency shift is modelled based on the initial slope $2f_{\rm L}\partial|\Delta f(T)|/\partial(1-T/T_c)|_{T\to T_c} = 3.96\times10^9\,{\rm Hz}^2$ measured in the $D = 0.2\,\mu$m cavity with 98%-specularly scattering walls and the calculated temperature dependence of the weak-coupling A phase energy gap. Here the initial slope is defined as the slope of a straight line fitted between $0.9T_c$ and $1.0T_c$.

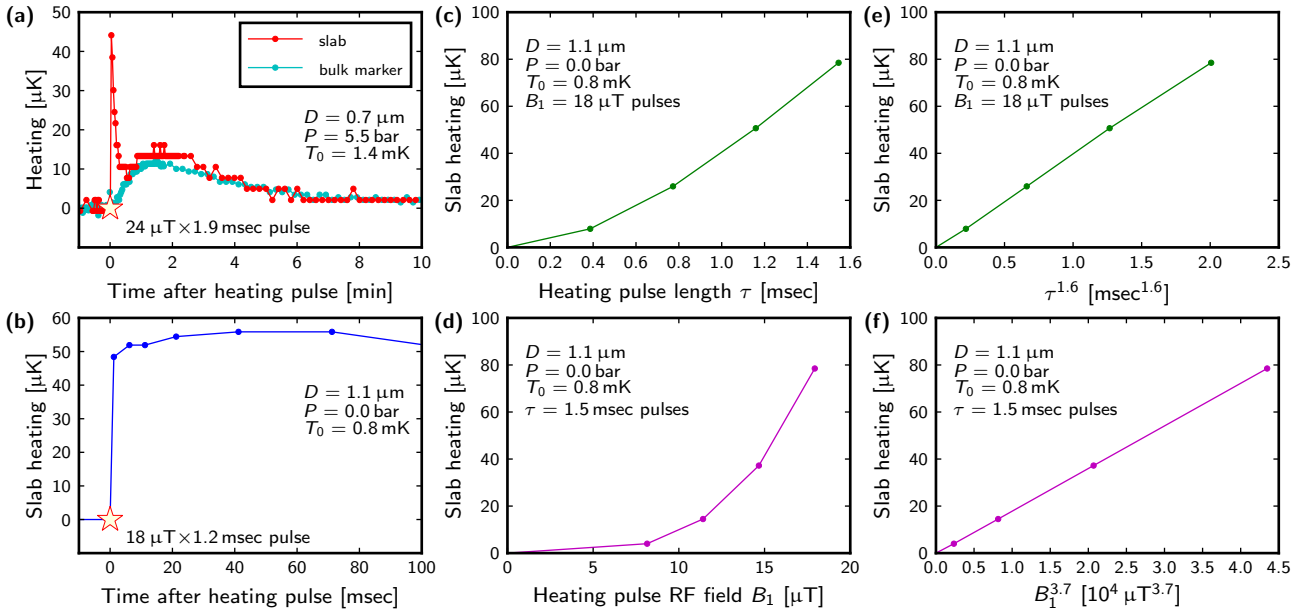

FIG. S3: Characterisation of heating of the confined ^{3}He by NMR pulses. Helium temperature is inferred from frequency shift probed regularly with small NMR pulses, while the heating is induced by large pulses, applied sufficiently far from Larmor frequency not to tip ^{3}He spins and rarely enough (once every 20 minutes) to let the sample cool down before it is heated again. (a) Heating in the slab and the "bulk marker" volume at the mouth of the fill line. Only the former rapidly warms up due to local heating we are concerned with; in addition both slowly respond to Joule heating of the metallic elements of the experimental setup, transmitted via the heat exchanger. Data from the $D = 0.7\,\mu$m slab with a large clearly-visible bulk marker [39]. The rest of the measurements were performed on the $D = 1.1\,\mu$m slab presented in this paper. (b) Time evolution of the slab temperature shortly after a large pulse. (c-f) Dependence of heating on the pulse duration τ and power of radio-frequency field B_1 measured 20 msec after pulses, when the slab reaches its highest temperature.

to the helium sample, is obtained from the suppression of bulk T_c, registered with NMR in the bulk ^{3}He marker at the mouth of the fill line. Fig. S2 demonstrates that such correction with a slightly different C is adequate for the present experiment, which utilised the same heat exchanger. In this work the NMR pulses were applied rarely enough to have no effect on C.

HEATING BY NMR PULSES

NMR experiments on superfluid ^{3}He under regular confinement in silicon-glass and fully-silicon cavities (Refs. [32, 39, 43] and this work) have manifested heating of an unidentified origin that couples to the confined liquid directly, Fig. S3a. Most heating occurs within 1 msec after the pulse (the duration of the probe NMR pulse plus the dead time of the NMR spectrometer), and the slab temperature is nearly constant for many msec afterwards, Fig. S3b. The dependence of the heating on duration τ and amplitude B_1 of the sine-wave pulses, Fig. S3c-f, is steeper than expected for linear dissipation ($\dot{Q} \propto \tau B_1^2$), especially when taking into account that specific heat of ^{3}He in the slab increases with temperature. This points towards an exotic origin of this parasitic effect.

In addition to the signatures shown in Fig. S3 we found that the heating is not resonant near the ^{3}He Larmor frequency, and that heating due to pulses with the initial 'antipulse', Fig. 2b, only depends on the total duration and amplitude, but not on the length of the 'antipulse' part.

As shown in Fig. S3b, the free induction decay after a large pulse with characteristic $T_2^* \approx$ 3-10 msec occurs at a nearly constant temperature, elevated above the

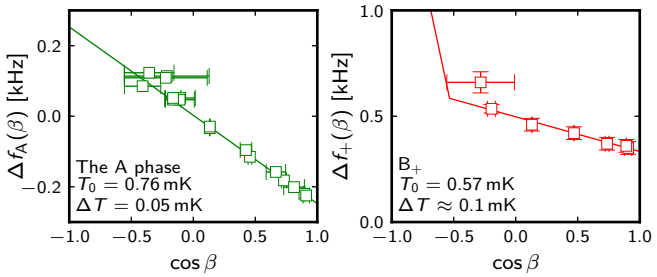

FIG. S4: NMR measurements on the A and B phase in $D = 1.1\,\mu$m slab with 18 μT×1.2 msec pulses. These pulses overheated the slab by ΔT above the temperature T_0 of the helium in the heat exchanger. Different tipping angles are achieved by applying the initial part of the pulse with a 180° phase shift, see Fig. 2b. In the dipole-unlocked A phase $\Delta f_A(\beta) \propto \cos\beta$, see [32] for $\Delta f_+(\beta)$.

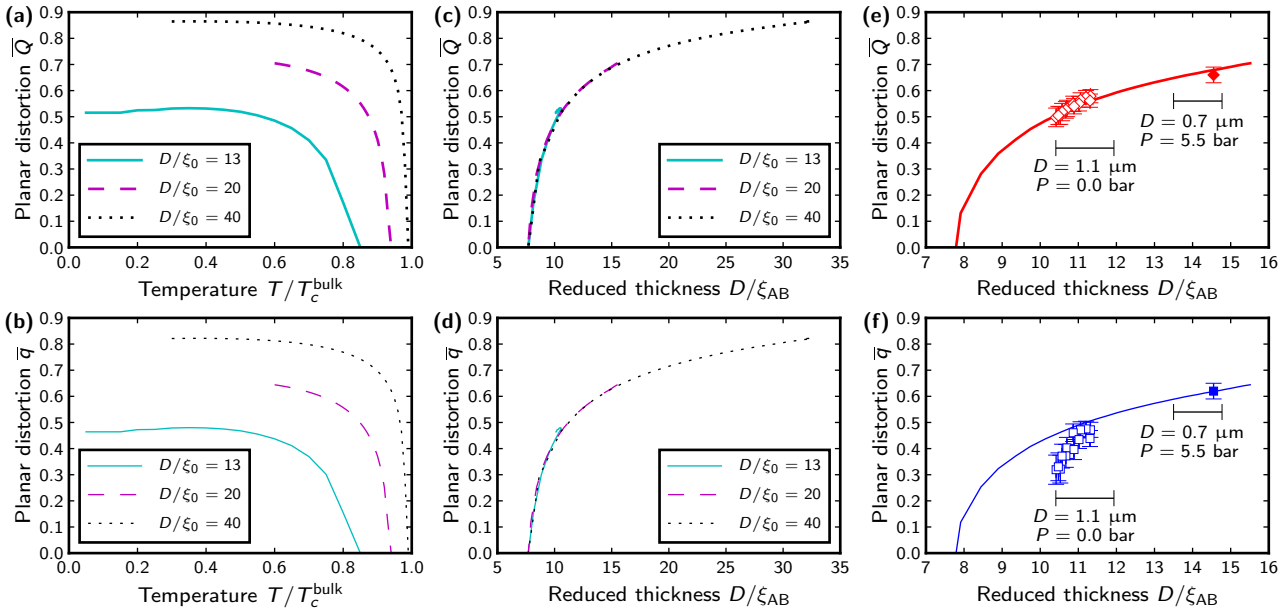

FIG. S5: Universal scaling of planar distortion parameters $\overline{q}$ and $\overline{Q}$ with reduced slab thickness $D/\xi_{\rm AB}$. (a-d) Calculations of planar distortion of spatially-invariant planar-distorted B phase at various D/ξ_0 [44]. See Eq. (S3) for the definition of the coherence length. (e-f) Comparison of these calculations to measurements on 0.7 μm slab (filled symbols) [32] and 1.1 μm slab (open symbols, showing together both warm-ups presented in Fig. 3). The horizontal bars represent the range of $D/\xi_{\rm AB}$ that can be probed in at given D and P limited by $T = T_{\rm AB}$ and $T = 0$.

temperature T_0 of helium in the heat exchanger and fill line. The use of 'antipulses', Fig. 2b, allows us to measure the NMR response as a function of tipping angle at a *constant* elevated temperature. This is illustrated in Fig. S4. We note that the strong frequency dependence of NMR tipping by 'antipulses', renders them unusable away from their carrier frequency. For this reason B_- is missing from Fig. S4, due to relatively large frequency range spanned by $\Delta f_-(\beta) \approx -1\,{\rm kHz} \times \cos(\beta)$. Probing B_+ above the magic angle β^* is equally problematic and was not studied here in detail.

In contrast the 0.7 μm slab was probed with groups of large pulses that caused different heating, restricting such measurements to the $T \lesssim 0.5T_c$ limit where the temperature dependence of the frequency shifts is weak [32].

In this work we demonstrated that tipping angles up to 60° could be reached with 8 μT×1.2 msec pulses, generating only $\Delta T \lesssim 10\,\mu{\rm K}$, small compared to the temperature range over which we probed the B phase gap distortion.

UNIVERSAL SCALING OF PLANAR DISTORTION

Within the Ginzburg-Landau regime, $T - T_c \ll T_c$, the effects of confinement on properties of the superfluid are determined by a single control parameter, the reduced thickness $D/\xi(T,P)$, where ξ is the coherence length. This universality breaks down at lower temperatures, i.e. see the supplementary of Ref. [39]. To study the A-B transition outside of the Ginzburg-Landau regime the coherence length has been defined as

$$\xi_\Delta(T,P) = \frac{\hbar v_{\rm F}(P)}{\Delta_{\rm B}(T,P)\sqrt{10}}, \qquad \text{(S2)}$$

were $v_{\rm F}$ is the Fermi velocity and $\Delta_{\rm B}$ is the bulk B phase gap. We observe that the weak-coupling quasiclassical calculations [44] of $\overline{q}(T)$ and $\overline{Q}(T)$ at different D collapse, see Fig. S5a-d, expressed as a function of D/ξ adopting a slightly different coherence length

$$\xi_{\rm AB}(T,P) = \frac{D_{\rm AB}(T,P)}{\pi\sqrt{6}}, \qquad \text{(S3)}$$

where $D_{\rm AB}(T,P)$ is the thickness of the slab at which the A to B transition occurs at temperature T and pressure P (the inverse of the $T_{\rm AB}(D/\xi_0(P))$ function [34]). Here we restrict the discussion to the calculations for a slab with specular boundaries and recognise that the pressure P only enters the weak-coupling calculations via the pressure dependence of the bulk transition temperature $T_c^{\rm bulk}(P)$ and the Cooper pair diameter $\xi_0(P) = \hbar v_{\rm F}(P)/2\pi k_{\rm B} T_c^{\rm bulk}(P)$. We find that $\xi_{\rm AB}/\xi_\Delta \to 1.0$ at $T \to T_c$ and $\xi_{\rm AB}/\xi_\Delta \to 1.1$ at $T \to 0$.

PLANAR DISTORTION: THEORY VS EXPERIMENTS

We compare the calculations discussed in the previous section with the NMR measurements of the planar distortion of the B phase in 0.7 and 1.1 μm slabs in Fig. S5e,f. The former, obtained at $P = 5.5\,\mathrm{bar}$ and $T = 0.6\,\mathrm{mK} = 0.4T_c^{\mathrm{bulk}}$ are in good agreement with the theory in terms of both $\overline{q}$ and $\overline{Q}$. This confirms that the strong coupling effects, known to increase with pressure, are not responsible for the reduced $\overline{q}$ presented in this paper, Fig. 3 and Fig. S5f.

QUALITATIVE DISCUSSION OF DOMAIN CONFIGURATIONS

In this section we compare possible structures of domains using the length of domain walls per unit area of the slab L/A as a figure of merit of the free energy gain due to formation of domain walls. We consider a two-dimensional problem of energetic stability of thin domain walls with hard-core repulsion at distance W. Dots are assumed to be circular. We find $L/A = 1/W$ for the stripe phase, $L/A = \pi/2W\sqrt{3} \approx 0.91/W$ for hexagonal lattice and $L/A = \pi/4W \approx 0.79/W$ for square lattice, listed in Fig. 4b-d. The fact that these numbers are all close to each other demonstrates that the free energy of 1D and 2D modulated states is nearly degenerate, and only a detailed calculation can reliably identify the lowest energy state, taking into account the gradual spatial variation of the order parameter components across the domain walls and the optimum shape of dots.

[32] L. V. Levitin, R. G. Bennett, E. V. Surovtsev, J. M. Parpia, B. Cowan, A. Casey, J. Saunders, Phys. Rev. Lett. **111**, 235304 (2013).

[34] Y. Nagato and K. Nagai, Physica B **284-288**, 269 (2000).

[39] L. V. Levitin, R. G. Bennett, A. Casey, B. Cowan, J. Saunders, D. Drung, Th. Schurig, and J. M. Parpia, Science **340**, 841 (2013).

[41] L. .V. Levitin, R. G. Bennett, A. Casey, B. Cowan, J. Saunders, D. Drung, Th. Schurig, J. M. Parpia, B. Ilic, and N. Zhelev, J. Low Temp. Phys. **75**, 667 (2014).

[42] V. Dotsenko and N. Mulders. J. Low Temp. Phys. **134**, 443 (2004).

[43] P. J. Heikkinen, A. Casey, L. V. Levitin, X. Rojas, A. Vorontsov, N. Zhelev, J. M. Parpia, and J. Saunders, *Tuning pair-breaking at the surface of topological superfluid ^{3}He* (unpublished).

[44] A. B. Vorontsov and J. A. Sauls, Phys. Rev. B **68**, 064508 (2003) and private communication.